



Convolutional Neural Network for Transmission Line Fault Diagnosis Based on Signal Segmentation Approach

Abdul Malek Saidina Omar¹, Ahmad Asri Abd Samat^{1,*}, Fasihah Faisal¹, Muhammad Khusairi Osman¹, Mohammad Nizam Ibrahim¹, Zakaria Hussain¹

¹ Electrical Engineering Studies, College of Engineering, Universiti Teknologi MARA, Cawangan Pulau Pinang, 13500 Permatang Pau, Pulau Pinang, Malaysia

ARTICLE INFO

Article history:

Received 11 May 2023

Received in revised form 7 September 2023

Accepted 20 September 2023

Available online 6 October 2023

Keywords:

Convolutional Neural Network; fault detection; signal segmentation; transmission line fault; white gaussian noise

ABSTRACT

Convolutional Neural Network (CNN) is a Deep Learning algorithm that can take in an input signal, assign importance (learnable weights and biases) to various aspects of the signals and distinguish between them. The CNN algorithm trains a sample and obtains a CNN model capable of identifying different fault types to analyse transmission line faults. Fault analysis methods typically require feature extraction to synthesise the relevant and non-redundant information from the raw signals. However, these traditional methods are time-consuming and inconsistent, and they can produce biased results due to the reliance on human expertise and experience. Hence, this research focused on developing an intelligent system for fault detection in a three-phase transmission line using CNN. This research aims to develop a CNN model for automatic fault detection in a three-phase transmission line and evaluate the performance of the CNN model for analysing transmission line faults. The three-phase transmission line model was developed using MATLAB-Simulink. CNN was implemented to detect transmission line faults. The performance of CNN based on the signal segmentation approach was evaluated through three different types of data: ideal and noise-added signal data. The simulation result shows good performance accuracy of 99.11% for the ideal case, 99.36%, and 99.39% for 20 dB and 30 dB noise-added cases, respectively. The result shows that a higher noise value in transmission line fault current could increase the performance of CNN. In conclusion, the utilisation of CNN based on a signal segmentation approach for transmission line fault analysis has showed promising performance.

1. Introduction

Deep learning and artificial intelligence techniques have recently received much attention in numerous sectors, and their applications in machine fault diagnostics are rapidly expanding [1]. In line with that, the Convolutional Neural Network (CNN) is emerging as a dominant method within artificial neural networks, especially in pattern recognition [2-4]. A CNN (ConvNet/CNN) is a Deep Learning algorithm that can take in an input image, assign importance (learnable weights and biases)

* Corresponding author.

E-mail address: ahmadasri759@uitm.edu.my

<https://doi.org/10.37934/araset.32.3.199216>

to various aspects or objects in the image and differentiate one from the other. The pre-processing required in a ConvNet is much lower than in other classification algorithms. CNNs have witnessed greater success by employing automated feature extraction and minimum signal-processing for fault diagnosis [2]. The transmission line is a long conductor with a special design (bundled) to carry a bulk amount of generated power at very high voltage from one station to another as per variation of the voltage level. Fault can be defined as the abnormal condition of the electrical system, which damages the electrical equipment and disturbs the normal flow of the electric current.

Feature extraction is commonly used in fault detection and diagnostic approaches to generate useful and non-redundant information from raw signals. Transmission line problems often contain important fault information within their current waveforms. Consequently, various techniques have been introduced to analyse these specific waveforms. However, picking out the finest attributes demands expert proficiency and could be extremely particular. Feature selection algorithms can be used to extract useful sets of features. Feature extraction increases the computational load of the diagnosis process and necessitates the availability of existing information before it can be applied to new systems. The transmission line fault-diagnosis algorithms in three-phase transmission lines have evolved similarly [5]. As discovered in many previous studies, traditional diagnostics consist of three stages: hand-crafted feature design, feature extraction and model training [3,6]. The transmission line fault diagnosis using classical methods involves additional processes. It requires complex signal-processing and feature extraction abilities. However, only professional and experienced persons are able to extract the feature [1]. There is no established theory to guide humans in selecting the right deep learning tools as it requires knowledge of topology, training method and other parameters. As a result, it is challenging for inexperienced individuals to adopt feature extraction. It requires a large amount of data to perform better than other techniques. Traditional fault diagnostic approaches rely heavily on traditional signal characteristics such as mean value, standard deviation, and kurtosis. Notwithstanding, some features may not be helpful in the detection process of faults in transmission lines. Signals still carry much information humans do not fully use [7]. Conventional fault detection requires much larger datasets with many more features. Thus, it takes a longer time to train the algorithm and more memory to work with data structures, leading to low fault detection accuracy [1].

To overcome this, several efforts have been made to create advanced approaches for extracting features indicative of fault progression and the corresponding machine-learning algorithms. The task of fault detection is completed prior to the fault location. With fault detection, the variations of electrical signals are commonly used as the startup criteria, and the if-then conditions can achieve the fault detection task. For the fault-location methods, Bayesian networks [8], expert systems [9], Petri Nets [10], fuzzy logic [11], and analytical models [12] are commonly cited in recent decades. However, these techniques still have certain drawbacks [13]. Out of these options, CNN has attracted more interest because of its specific local shared weights arrangement, which offers a considerable computational benefit. Chen *et al.*, [5] proposed combined fault location and classification to diagnose power transmission line faults with integrated feature extraction. Han *et al.*, [13] presented fault diagnosis of power systems using visualised similarity images (VSI) and improved convolution neural networks (ICNN). Paul *et al.*, [14] developed fault classification in transmission lines using wavelet and CNN. Jamil *et al.*, [15] also suggested fault detection and classification in electrical power transmission systems using artificial neural networks. Benson *et al.*, [16] presented a modified CNN for detecting faults during power swings in transmission lines. Kim *et al.*, [17] implemented CNN for gear fault diagnosis based on a signal segmentation approach. CNNs overcome the shortcomings of conventional expert systems and reduce reliance on prior expert knowledge [13]. The main advantage is that it allows minimal engagement of signal-processing and enables automated

extraction of optimal features that directly represent the fault type of a three-phase transmission line system [18]. Compared with the traditional methods, the proposed CNN-1D exhibits quick and accurate fault detection with better performance [19].

Previously, the accuracy of the CNN model was most commonly checked via cross-validation using data for normal and faulty conditions, in which a portion of the data is arbitrarily chosen for training and the remaining for testing. Most of the reported data had outstanding accuracies, suggesting its potential for fault diagnosis. However, the performance may not be the same in practice for the transmission line fault since there might be noise in the three-phase transmission line fault. Furthermore, the fault for the test may appear at different locations with different fault types from those of the training. To date, CNN studies in transmission line fault diagnostics have never taken this into account, which is a significant concern in terms of practical application. To solve this issue, this paper offers a novel technique that involves segmenting the original signal into those at each fault and unfaulted transmission line segment. Subsequently, the CNN is implemented for fault detection. This research aims to develop an intelligent system for fault detection in three-phase transmission lines using CNN. The objectives are to model a three-phase transmission line for fault signal generation using MATLAB-Simulink, to develop a CNN for automatic fault detection in three-phase transmission lines and to evaluate the performance of the proposed method using accuracy and F1-score. The motivation here is to ensure that the input data is provided appropriately so that the type of transmission line does not influence the fault information.

This paper proposes a CNN model for diagnosing three-phase transmission lines based on signal segmentation. This research includes 1D-CNN, a three-phase transmission line fault model, fault analysis, intelligent system development and fault types. This study focuses on the application of 1D-CNN (1D-CNN) in three-phase transmission line fault detection. The 1D-CNN is proposed as this architecture has successfully processed the transmission line signal and achieved better accuracy than other methods. Moreover, fault detection is the first and the most important part of all three parts of fault analysis. The fault detection analysis will influence the outcome of fault location and fault classification in transmission lines. Therefore, this research emphasises the dominant part of fault analysis: fault detection. The detected faults were classified into faulted and unfaulted transmission lines. There are two main types of faults: series (open conductor faults) and shunts (short circuit faults). For the system development, a Simulink Model for three-phase transmission line and 1D-CNN(1D-CNN) architecture was developed for medium distance transmission line system. The simulations were performed using MATLAB and Simulink to obtain all the results related to fault detection.

CNN, which was the dominating technique in the field of image and voice recognition, has proven enormously effective in a variety of practical applications. Convolutional networks are neural networks that utilise convolution, a linear operation, instead of ordinary matrix multiplication in at least one of its layers. The intention behind CNN's design is to leverage two major advantages. First, CNN is relatively easier to train and has fewer parameters to learn than the traditional fully connected neural networks, which have more hidden layers. Second, because of the unique benefit of convolution operation over 2D space, CNN is ideal for two-dimensional (2D) picture inputs. CNN usually consists of two parts. One is the feature extractor, which learns features from raw data automatically. The other is a trainable, fully connected multi-layer perceptron (MLP), which performs classification based on the learned features from the previous part. Feature extractor consists of two layers: convolutional and subsampling. The former convolutional layer has a number of filters called learnable kernels, which involve the previous layer's feature maps with filters and are activated by the activation function to form the output feature map. The process of convolutional layers can be expressed as follows

$$x_j^l = f \left(\sum_{i \in M_j} x_j^{l-1} * k_{ij}^l + b_j^l \right) \quad (1)$$

where M_j represents a selection of input maps; l is the l_{th} layer in a network; k is a $S \times S$ matrix, where S is the size of convolutional kernels; f is an activation function such as the hyperbolic tangent, sigmoid, or rectified linear unit (ReLU) function. The latter subsampling layer, also known as the pooling layer, replaces the output of the filter with a summary statistic of the nearby outputs. It makes the output less sensitive to the small translation of input data and helps to reduce the resolution of output from the convolutional layers. The pooling function can be max, average, L^2 norm, or the weighted average pooling within the rectangular pooling block. The most commonly used function is the max pooling, which can be computed as follows

$$P_j^l = \max_{x_j^l \in S} x_j^l \quad (2)$$

where P_j^l is the output of max pooling layer l , S is the pooling block size, and x_j^l is the output from the convolutional layer. Once the feature extractor is established, fully connected Multi-layer Perceptron (MLP) and SoftMax layers are added for classification [17].

The rest of this paper is organised as follows: Section I explains the overview of CNN; Section II depicts the three-phase transmission line parameters value; Section III describes the signal segmentation approach based on CNN and discusses the results for ideal case and noise-added cases; and finally, Section IV presents the conclusion of this paper.

2. Methodology

2.1 Three-Phase Transmission Line Fault

A three-phase transmission line model was developed using MATLAB-Simulink. MATLAB-Simulink was utilised to simulate the three-phase transmission line model, serving as the benchmark for fault detection topology. It encompasses relevant components of electric power systems such as PowerGUI, Three-Phase Source, Three-Phase PI Section Line, Three-Phase V-I Measurement, Three-Phase Fault, Scope Voltage and Scope Current. The parameters and values used in the three-phase transmission line model are displayed in Table 1.

Table 1
 Three-phase transmission line parameters value

Parameters	Value
Length (L)	100 km
Frequency (F)	50Hz
Voltage rating (S1 and S2)	400kV
Zero sequence impedance (Z0)	0.0461 + j0.8340 Ω/km
Positive sequence impedance (Z1)	0.0154 + j0.2783 Ω/km, [0.01273 0.3864]
Zero sequence capacitance (C0)	4.355 nF/km
Positive sequence capacitance (C1)	13.065 nF/km, [12.74e ⁻⁹ 7.751e ⁻⁹]

In this research, the voltage rating used was 400kV phase voltage. The phase voltage should be multiplied to the square root of 3 to get the line voltage. Hence, a 400 kV three-phase circuit means that each of the 3 lines carries 230 kV. The frequency used was 50 Hz. The medium-distance three-phase transmission line ranges from 80 km to 100 km. In this model, two values of sequence impedance and capacitance are used. The zero and positive sequence impedance are 0.0461 +

$j0.8340 \Omega/\text{km}$ and $0.0154 + j0.2783 \Omega/\text{km}$, $[0.01273 \ 0.3864]$ respectively. On the other hand, the zero and positive sequence capacitance are $4.355 \text{ nF}/\text{km}$ and $13.065 \text{ nF}/\text{km}$, $[12.74e^{-9} \ 7.751e^{-9}]$ respectively.

2.2 Signal Segmentation Approach Based on CNN for Transmission Line Fault Diagnosis

A signal segmentation-based approach is proposed to diagnose the transmission line condition independent of fault type and presence of noise. This approach is required because it is essential to ascertain the fault type, especially considering the vulnerability of transmission line faults to high-noise conditions. The idea is to divide the original raw signal over a single rotation into the segments at each fault type. Figure 1-3 shows the flowchart of the method, which is composed of three steps: Figure 1(a) and 1(b) for signal processing, Figure 2 for signal segmentation, and Figure 3 for 1D-CNN implementation. In the first step, the signal is pre-processed by angular resampling, followed by time synchronous averaging (TSA) to remove the inherent random noise and average the data segments of successive 4 cycles over a single cycle. In the second step, which is the signal segmentation, the signal is further divided into segments corresponding to the interval of transmission line fault current using the autocorrelation function, as presented in the next section. In the third step, the 1D CNN is implemented to classify the fault, which is comprised of three sub-steps:

- i. Convolutional + pooling operations over the corresponding layers are performed to extract features automatically.
- ii. Fully connected layers are used for classification, and
- iii. The softmax layer is finally added to convert the result of CNN classification into probability.

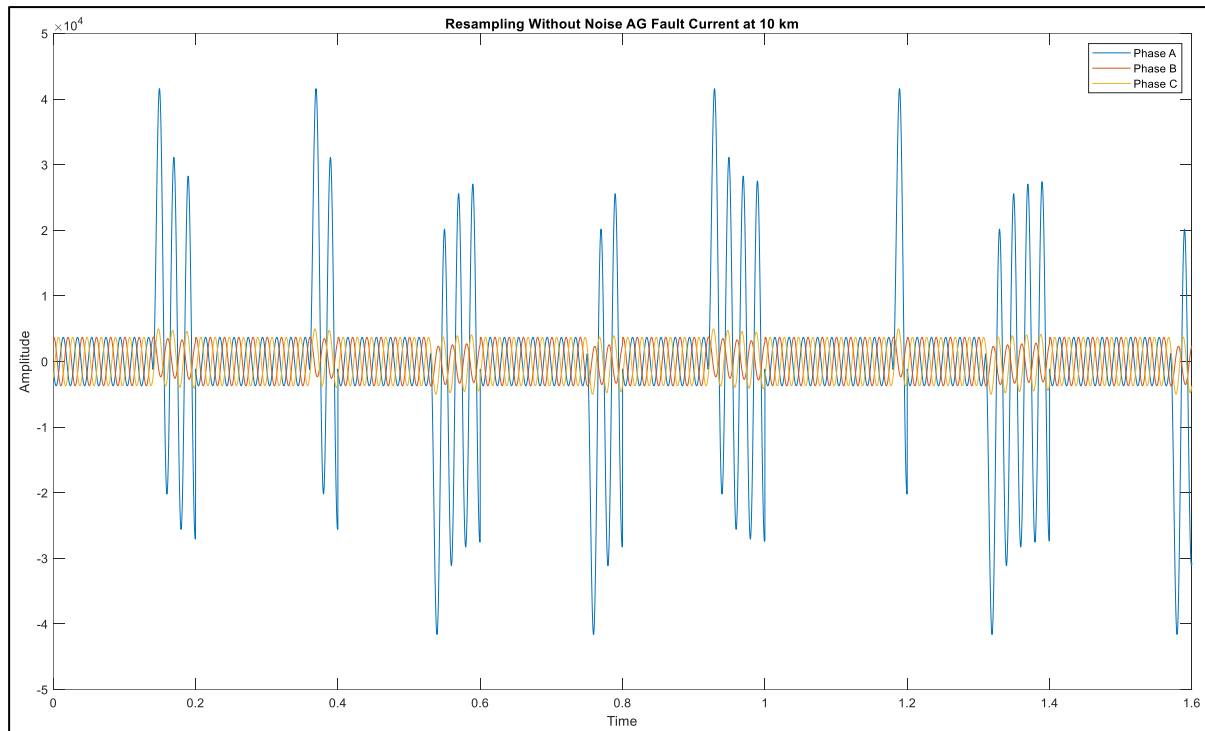
3. Results and Discussion

3.1 Signal Resampling

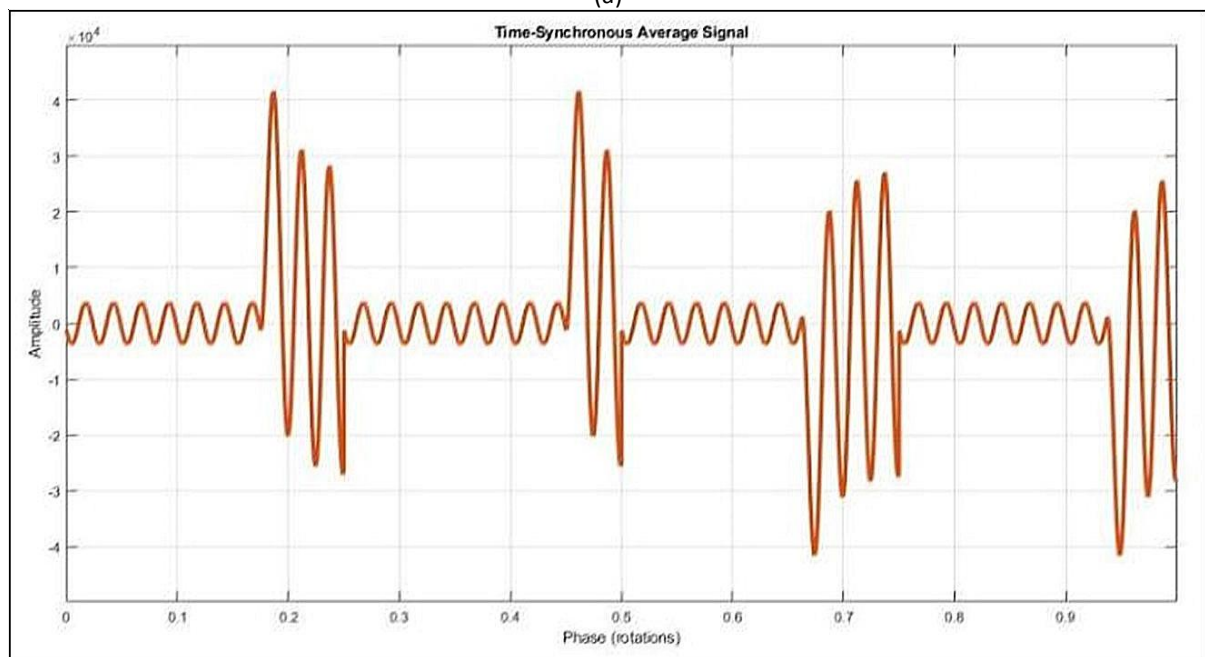
Resampling is the process of changing the sampling rate of an existing signal. The resample function is designed to convert sample rates to higher or lower. A new signal should keep all information contained in the original signal. It is the method of removing noise and unwanted data or eliminating variations that arise while acquiring a signal without evading essential information. It also aids in eliminating unwanted artefacts from the transmission line signal and makes it suitable for further processing. The signal-processing by angular resampling is implemented to pre-process the transmission line signal.

3.2 Time Synchronous Averaging

Time-synchronous averaging (TSA) is a signal-processing technique that extracts periodic waveforms from noisy data. It is an essential algorithmic tool for determining the condition of transmission line signals. Time synchronous average resamples the vibration data synchronously with a fault. The TSA is well suited for transmission line fault analysis, where it allows the vibration signal of the fault current under analysis to be separated from other signals and noise sources in the transmission line that are not synchronous with that signal. Once all the time averaging is completed, the transmission line signal correlated to the pulse signal should remain, and any uncorrelated signals should average towards zero. Hence, the implementation of signal-processing via time synchronous averaging aims to average the segment's transmission line fault into successive 4 cycles.



(a)



(b)

Fig. 1. (a) Signal resampling, (b) time synchronous averaging

3.3 Signal Segmentation Through Autocorrelation Function

The autocorrelation function (ACF) defines how data points in a time series are related, on average, to the preceding data points. In other words, it measures the self-similarity of the signal over different delay times. The signals are processed to achieve segmentation for each unfaulted and faulted transmission line current. To this end, the autocorrelation function is introduced, which is the correlation between original n^{th} signal $X(n)$ and its delayed signal with lag t , and is given by

$$R_{xx}(\tau) = E[X(n)X(n + \tau)] \tag{3}$$

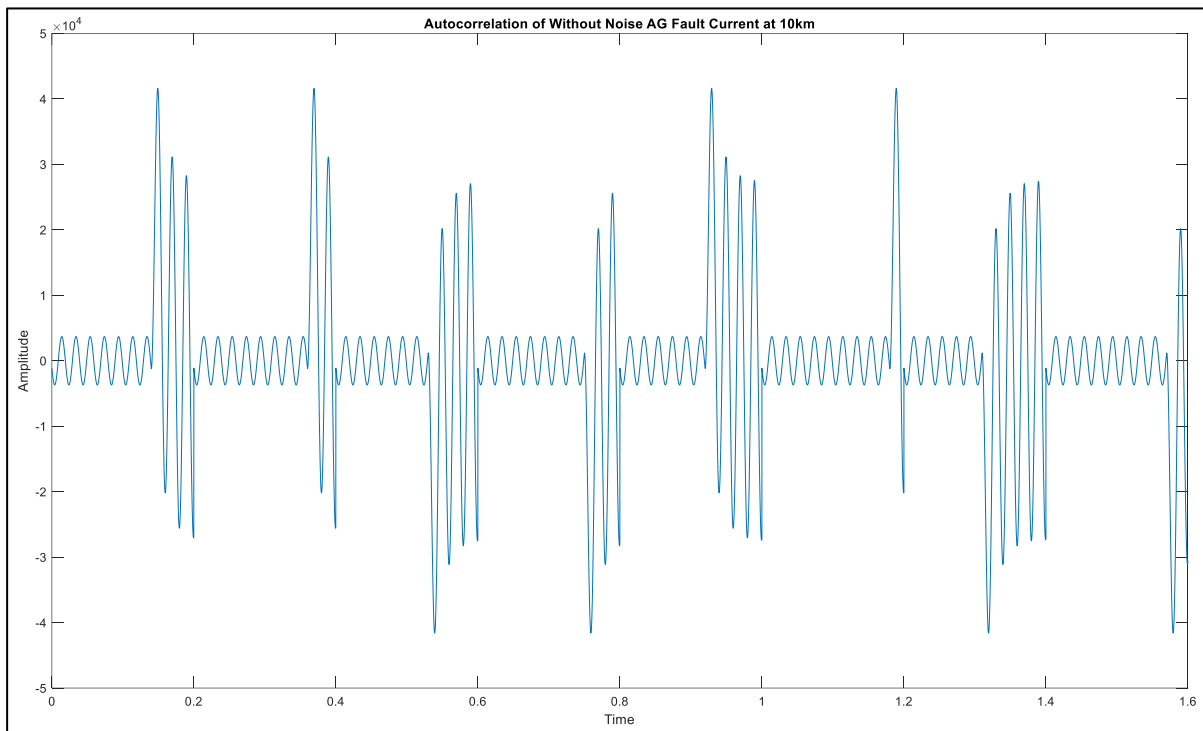


Fig. 2. Signal segmentation using autocorrelation to divide into the fault segments

The interval between adjacent maxima of the autocorrelation function defines a signal segment over a fault. As a result, 20 segments for the output transmission line are obtained in which the number represents the current in the input and output transmission lines, both in faulted and unfaulted states.

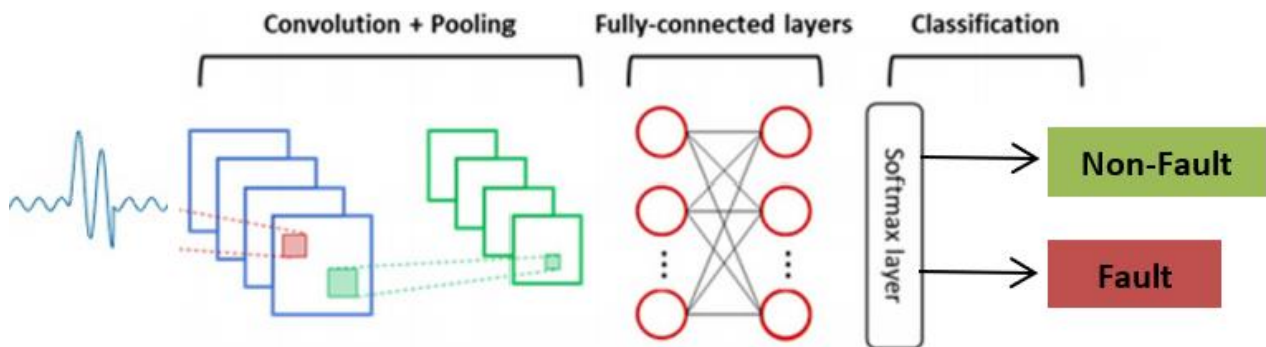


Fig. 3. 1D-CNN to detect the faults using the segmented data sets

Figure 4-6 show the snapshots of the segmented ideal, with 20 dB noise and 30 dB noise signals obtained by this process, which are unfaulted and faulted, respectively. Note that the signal is normalised with zero mean and unit variance for standardisation. As in the ideal case signal, the signal in Figure 4 shows a smoother waveform compared to Figure 5 and 6, showing the distortion in the segmented signal. For the distortion in Figure 5 and 6, however, the difference is less noticeable, exhibiting a monotonic sine wave, which makes it hard to distinguish. As for the case of the 20 dB noise signals, as shown in Figure 5, disturbance characteristics are also visible to some degree with the transmission line fault current signal due to a large amount of high-frequency noise. Hence, the segmented data sets are applied to the CNN model to capture this difference automatically.

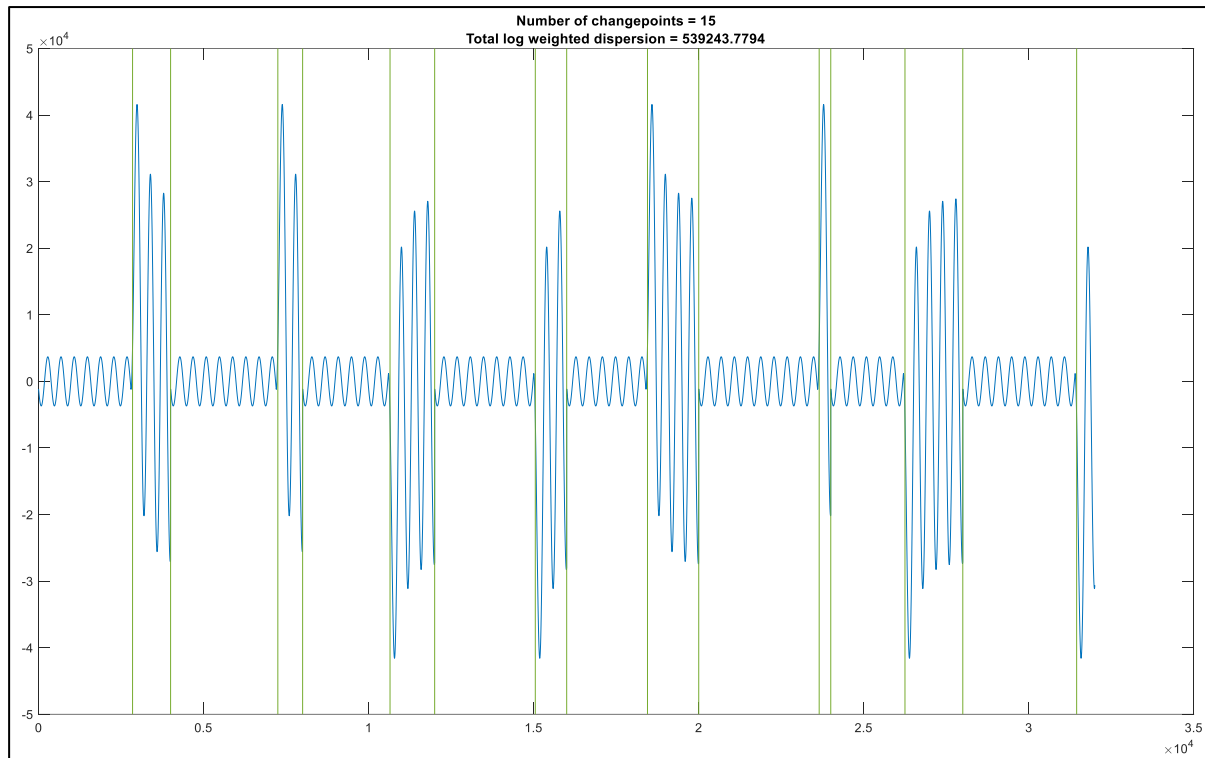


Fig. 4. Segmented ideal signal

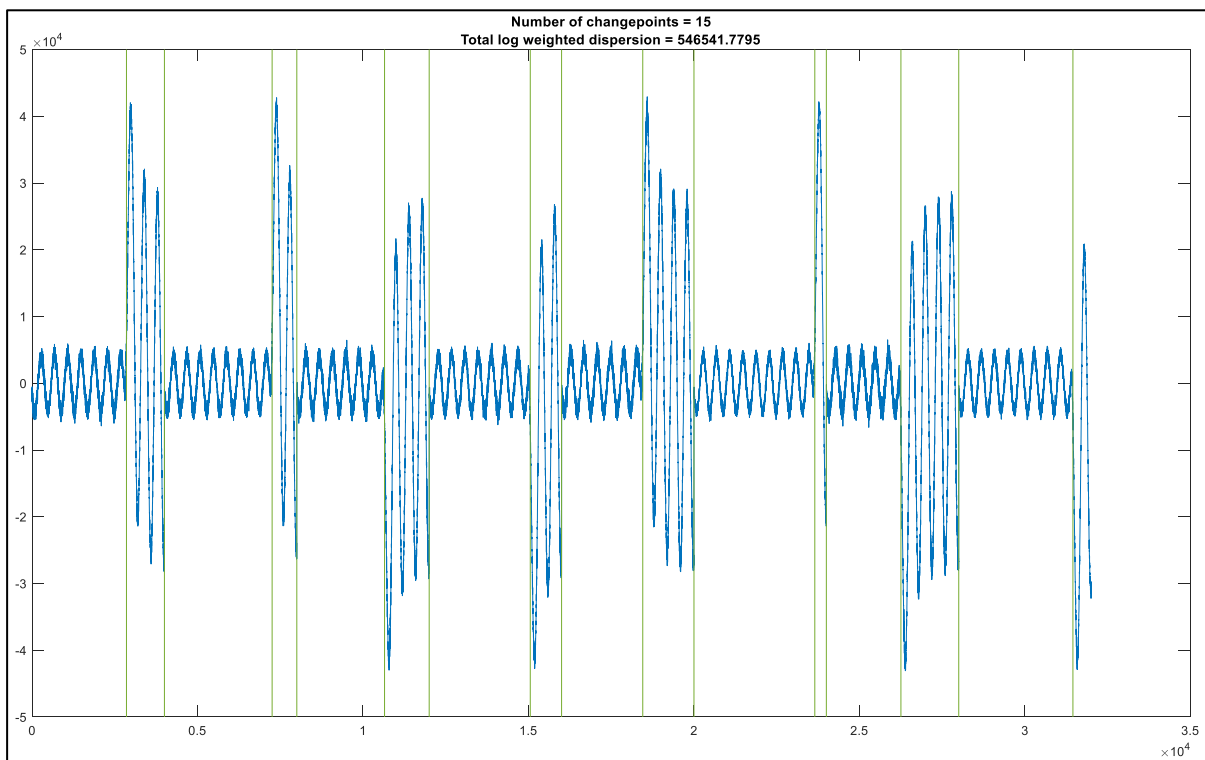


Fig. 5. Segmented 20 dB noise

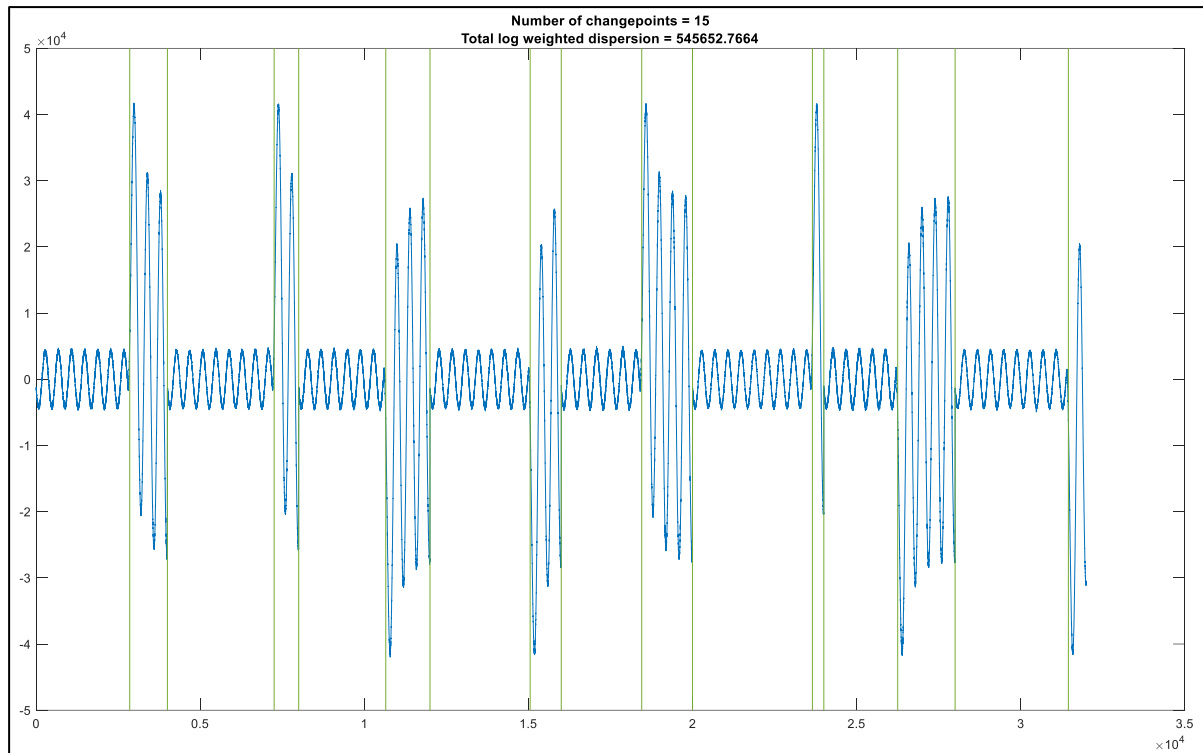


Fig. 6. Segmented 30 dB noise

3.4 Data Preparation

Ideally, 20 dB noise and 30 dB fault current of the noise transmission line is measured during 8 cycles of 4 different fault types with the sampling rate of 50 Hz. Multiple data sets are generated by different simulation times and fault locations for each 10 km, up to 100 km. Thus, 12 data sets are obtained for the transmission line fault current, with 4 different fault types from each parameter. Each of the data sets contains another 10 data with different fault locations. The different fault location data was then divided into training and testing data. As mentioned, the whole number of data sets is 10 before segmentation, divided by 8 and 2 for training and testing purposes, respectively. The data sets are labelled as 1, 2, and 3, representing faulted, 20 dB, and 30 dB noise, respectively.

3.5 Performance of Convolutional Neural Network

Once the data sets become available, the sets are usually divided into training and testing data sets. During the training, the optimum CNN design is sought by employing cross-validation to identify the best parameters of the model. For this purpose, the training sets are further divided into the training and validation sets. In the validation, the average performance is evaluated using the trained model by choosing the validation sets several times at random. The experiments are conducted for several candidate parameters to ascertain the model with the best performance. The trained CNN model is then applied to the testing data sets to evaluate the classification's performance.

As shown in Table 2(a), the confusion matrix is usually employed for this, where the row and column represent the predicted class from the model and its true class, respectively. The diagonal components signify data that are classified correctly, whereas the off-diagonal components describe misclassified data. TP and FP are the numbers of true-positive and false-positive predictions, and FN and TN are the numbers of false-negative and true-negative predictions, respectively. In order to

assess the performance via this, several standard terms can be defined, such as accuracy, precision, recall, and F1-score, as explained in the following equations

$$Recall = \frac{TP}{TP+FN} \tag{4}$$

$$Precision = \frac{TP}{TP+FP} \tag{5}$$

$$Accuracy = \frac{TP+TN}{TP+FP+FN+TN} \tag{6}$$

$$F1 - score = \frac{2(Recall)(Precision)}{Recall+Precision} \tag{7}$$

The accuracy, recall, and precision are presented in Table 2 at each location of the matrix. While accuracy is usually adopted in most diagnostic studies, it is not useful when there is a large class imbalance between the normal and faulty data sets, as seen in our study. The reason is that accuracy tends to predict the value of the majority class for all predictions, resulting in high classification accuracy, which is called the "Accuracy Paradox." The paradox can be demonstrated via two cases, as presented in Table 2(b), where the accuracies of cases A and B are the same at 95%. However, the first has missed most of the positive (fault) classes (45 of 50) as opposed to the second (5 of 50), which is obviously unacceptable for fault detection. To overcome this, the F1-score, the harmonic average of the recall and precision as defined in equations (4) and (5), is employed as a supplement. The closer the F1-score is to 1, the more effective it is in reducing false predictions. The values are 0.167 and 0.643, which show that the second is much better.

Table 2
 Confusion matrix and the illustrative examples: (a) elements of the confusion matrix and (b) two cases of confusion matrix

		Predicted class			
Model	-	+			
True	-	TN	FP		
class	+	FN	TP	Recall	
				Precision	Accuracy
(a)					

		Predicted class					
Case A	-	+		Case B	-	+	
True	-	945	5	True	-	905	45
class	+	45	5	class	+	5	45
			0.5	0.95			0.9
							0.95
(b)							

The confusion matrix is applied to this study's two-class (non-fault and fault) problems. The matrix is modified to include the two classes in the row and column. The recall and precision are then calculated by considering the data as the two classes, where the positive class represents the non-fault category and the negative class represents the faulted transmission line based on its type of fault. As a result, four confusion matrices were obtained, representing the single line-to-ground fault, double line fault, double line-to-ground fault and triple line fault. The accuracy rate and F1-scores are then obtained for each type of transmission line fault.

3.5.1 Performance of CNN for ideal case

Table 3 shows 4 confusion matrices of ideal transmission line fault current. The recall, precision, accuracy and FI-score of the ideal transmission line fault are shown in Table 4. In this case, the highest and the lowest recall are computed by ABC and AB faults which are 0.9995 and 0.9974, respectively. Furthermore, AG and ABG faults share the same total number of fault recall at 0.9988. These findings can be associated with selecting false-negative predictions as one of the necessary parameters to calculate the recall. As shown in Table 3 and Table 4, it can be seen that the recall will increase as the false-negative predictions decrease. On the other hand, AB and ABC faults have the lowest and the highest precision at 0.9810 and 0.9955 each. Moreover, the ABG fault has a marginally lower precision of 0.9884 compared to 0.9919 of the AG fault. It is noted that the false-positive predictions correlated highly to the fault precision. These results clearly indicate that the higher the false-positive predictions, the lower the fault precision.

In this study, the highest and the lowest accuracy were given by ABC and AB faults, respectively. In addition, AG fault has slightly higher accuracy at 0.9933 than 0.9906 in ABG fault. As equation (6) mentioned, the fault accuracy is strongly related to the true-positive and true-negative predictions. The FI-score depends on the calculated recall and precision of each fault. As such, it can be observed that the highest FI-score is incurred by ABC fault, followed by AG, ABG and AB fault. In a nutshell, the average accuracy and FI-score of the ideal transmission line fault are 0.9911 and 0.9939 each. Hence, it is worth mentioning that the average fault accuracy and FI-score for the ideal transmission line fault current reached levels that were deemed satisfactory, surpassing 99%.

Table 3

Confusion matrix of Ideal Case: a) single line-to-ground fault, b) double line fault, c) double line-to-ground fault and d) triple line fault

		Predicted class				Predicted class	
Without noise	AG	NF		Without noise	AB	NF	
True class	AG	8620	188	True class	AB	8359	449
	NF	28	23165		NF	60	23133
(a)				(b)			
		Predicted class				Predicted class	
Without noise	ABG	NF		Without Noise	ABC	NF	
True class	ABG	8536	272	True class	ABC	8704	104
	NF	28	23165		NF	11	23182
(c)				(d)			

Table 4

Recall, precision, accuracy, and fi-score of the ideal case

Fault type	Recall	Precision	Accuracy	FI-score
SLG (AG)	0.9988	0.9919	0.9933	0.9953
DL (AB)	0.9974	0.9810	0.9841	0.9891
DLG (ABG)	0.9988	0.9884	0.9906	0.9936
TL (ABC)	0.9995	0.9955	0.9964	0.9975
		Average	0.9911	0.9939

3.5.2 Performance of CNN for 20 dB noise

Table 5 exhibits 4 confusion matrices of the 20 dB fault current of the noise transmission line. Table 6 depicts the recall, precision, accuracy and FI-score of the 20 dB noise transmission line fault. In this study, ABC and AG faults recorded the lowest and the highest recall at 0.9989 and 0.9994, respectively. In addition, the ABG fault has a slightly lower recall of 0.9990 compared to 0.9992 for the AB fault. This situation is due to the fact that the recall decreases with the increase of false-negative predictions, as presented in Table 5. Besides, the highest and the lowest precisions were given by ABG and ABC faults which are 0.9965 and 0.9851, respectively. Meanwhile, the AB fault has a fractionally higher precision at 0.9936 than 0.9934 in the AG fault. As presented in Table 3 and Table 6, it can be seen that precision generally improves as the number of false-positive predictions decreases.

In this case, ABC and ABG faults computed the lowest and the highest accuracy at 0.9882 and 0.9967, respectively. Moreover, AB fault has marginally lower accuracy at 0.9947 compared to 0.9948 of AG fault. Notably, the values of true-negative and true-positive predictions of each fault type strongly influence fault accuracy. This statement is reflected in the theoretical calculations of accuracy in equation (6). Additionally, the FI-score value of each fault type was generated by both recall and precision, as shown in equation (7). That is why the ABG fault exhibits the highest FI-score among other faults. Due to the balance value difference between recall and precision in AG and AB faults, respectively, these faults produce the same FI-score at 0.9964. In short, the average accuracy and FI-score of 20 dB noise transmission line fault are 0.9936 and 0.9956, respectively. Therefore, it is worth mentioning that the average fault accuracy and FI-score of 20 dB fault current of the noise transmission line achieved satisfied values above 99%.

Table 5

Confusion matrix of 20 dB noise: a) single line-to-ground fault, b) double line fault, c) double line-to-ground fault and d) triple line fault

		Predicted class				Predicted class	
20-dB noise		AG	NF	20-dB noise		AB	NF
True class	AG	8655	153	True class	AB	8658	150
	NF	13	23180		NF	19	23174
(a)				(b)			
		Predicted class				Predicted class	
20-dB noise		ABG	NF	20-dB noise		ABC	NF
True class	ABG	8726	82	True class	ABC	8457	351
	NF	24	23169		NF	26	23167
(c)				(d)			

Table 6

Recall, precision, accuracy, and fi-score of 20 dB noise

Fault type	Recall	Precision	Accuracy	FI-score
SLG (AG)	0.9994	0.9934	0.9948	0.9964
DL (AB)	0.9992	0.9936	0.9947	0.9964
DLG (ABG)	0.9990	0.9965	0.9967	0.9977
TL (ABC)	0.9989	0.9851	0.9882	0.9920
Average			0.9936	0.9956

3.5.3 Performance of CNN for 30 dB noise

Table 7 exhibits 4 confusion matrices of 30 dB fault current of the noise transmission line. The recall, precision, accuracy and FI-score of the 30 dB noise transmission line fault are shown in Table 8. In this case, the highest and the lowest recalls were computed by ABC and AG faults which are 0.9998 and 0.9982, respectively. Furthermore, the ABG fault has a marginally higher recall of 0.9991 compared to 0.9989 for the AB fault. It can be observed that the false-negative predictions are highly correlated to fault recall. These results indicate that the lower the false-negative predictions, the higher the fault recall will be. Apart from that, AG and AB faults recorded the lowest and the highest precisions at 0.9914 and 0.9941, respectively. Moreover, the ABG fault has a slightly lower precision at 0.9915 than 0.9934 in the ABC fault. It was due to false-positive prediction being one of the vital parameters to calculate the precision. It can be seen that as the false-positive predictions increase, the precision will decrease.

In this study, the highest and the lowest accuracy was given by ABC and AG faults at 0.9950 and 0.9924, respectively. In addition, the AB fault has a slightly higher accuracy at 0.9949 compared to 0.9931 of the ABG fault. As stated in equation (6), the fault accuracy is strongly influenced by the values of true-negative and true-positive predictions of each fault type. The FI-score depends on the calculated recall and precision of each fault. This situation is reflected in the theoretical calculations as shown in equations (7), whereas the value of recall and precision plays an important role in FI-score. That is why the ABC fault was attributed to the highest FI-score, followed by AB, ABG and AG faults. In brief, the average accuracy and FI-score of the 30 dB noise transmission line fault are 0.9936 and 0.9956, respectively. Thus, it is worth stating that the average fault accuracy and FI-score of 30 dB fault current of the noise transmission line achieved satisfied values above 99%.

Table 7
 Confusion matrix of 30 dB noise: (a) single line-to-ground fault, (b) double line fault, (c) double line-to-ground fault and (d) triple line fault

		Predicted class				Predicted class	
30-dB noise		AG	NF	30-dB noise		AB	NF
True	AG	8606	202	True	AB	8670	138
class	NF	41	23152	class	NF	26	23167
(a)				(b)			
		Predicted class				Predicted class	
30-dB noise		ABG	NF	30-dB noise		ABC	NF
True	ABG	8610	198	True	ABC	8654	154
class	NF	22	23171	class	NF	5	23188
(c)				(d)			

Table 8
 Recall, precision, accuracy, and fi-score of 30 dB noise

Fault type	Recall	Precision	Accuracy	FI-score
SLG (AG)	0.9982	0.9914	0.9924	0.9948
DL (AB)	0.9989	0.9941	0.9949	0.9965
DLG (ABG)	0.9991	0.9915	0.9931	0.9953
TL (ABC)	0.9998	0.9934	0.9950	0.9966
		Average	0.9939	0.9958

3.5.4 Comparison of CNN fault detection performance between different parameters

In this study, three different parameters of transmission line fault were introduced to investigate the performance of CNN. A deep neural network often indicates reduced accuracy in a real-world detection task. The problem is that real-world transmission lines often include noise or quality loss. The transmission line fault diagnosis based on the signal segmentation approach was proposed to achieve a stable fault detection performance in a real-world task. Figure 7 compares CNN performance for ideal, 20 dB, and 30 dB noise. In this case, the average accuracy of ideal, 20 dB noise and 30 dB noise were computed to be 99.11%, 99.36% and 99.39%, respectively. Meanwhile, the values of 99.39%, 99.56% and 99.58% represent the average FI-score of ideal, 20dB noise and 30dB noise, respectively.

The most common transmission line pre-processing methods were chosen to investigate the integrity of the input signal pre-processing. The pre-processing method produced significant improvement and proved successful in the fault diagnosis. As mentioned in Section III, signal resampling removes the noise, unwanted data and eliminates variations that arise during the acquisition of a signal without evading essential information. Time synchronous averaging is well suited for transmission line fault analysis, where it allows the vibration signal of the fault current under analysis to be separated from other signals and noise sources in the transmission line that are not synchronous with that signal.

The 20 dB and 30 dB noises contain fewer noise signals after the pre-processing process, which are expected to be robust to quality distortion. This hypothesis was based on the idea that the recall value, precision, average accuracy and average FI-score of the transmission line fault increase even after a quality loss. Moreover, because this approach utilised the signal segmentation using the autocorrelation function as an augmented feature of the original signal, the noise did not reduce the accuracy of the original transmission line fault signal while achieving better records of all types of quality distortion. The discovery is meaningful since the model did not depend on the type of noise used in the training phase. Therefore, this architecture could be interpreted as a generalised model for quality loss.

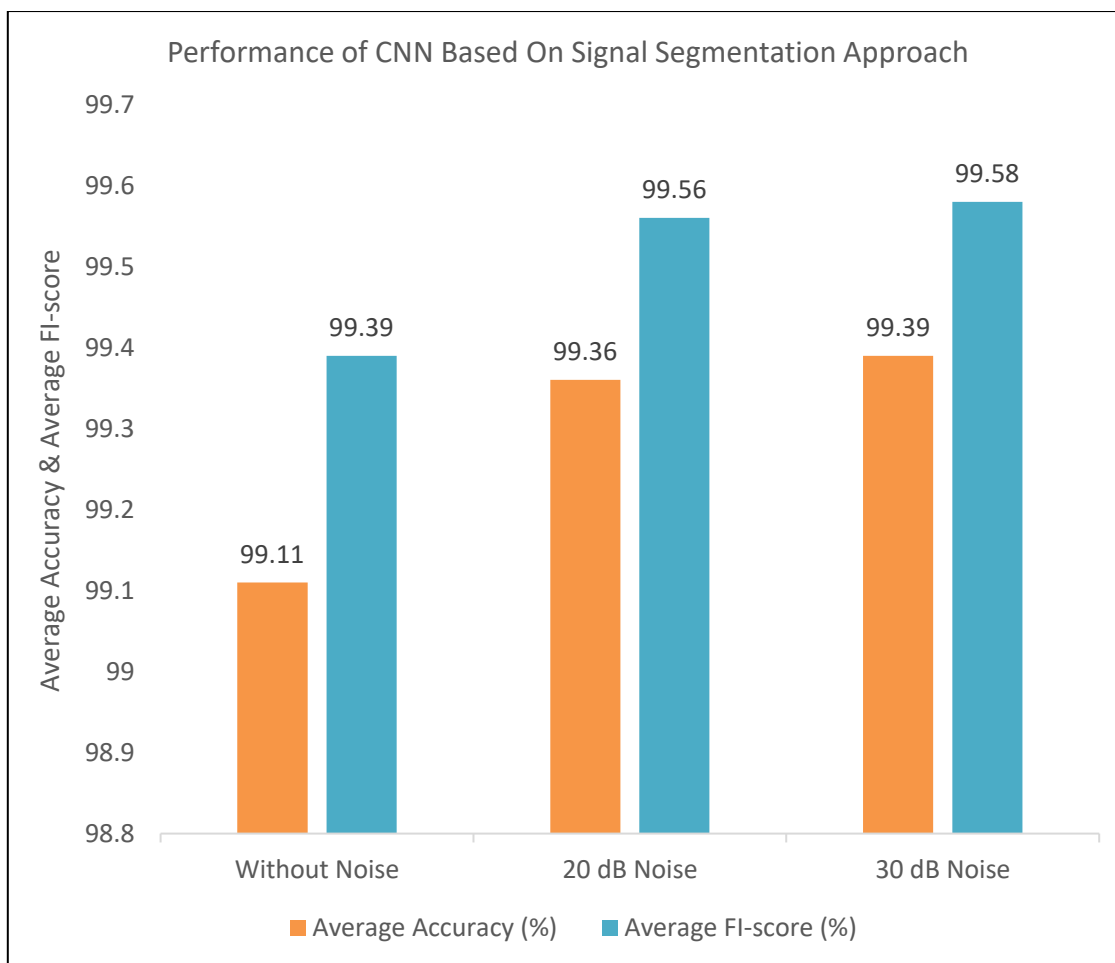


Fig. 7. Performance of CNN Based on signal segmentation approach

3.5.5 Comparison of CNN fault detection performance with alternative existing methods

Besides comparing the performance of CNN among different parameters, the fault diagnosis results are compared to alternative approaches [20,21]. In Ref. [20], S-transform was used as the pre-processor for feature extraction and deterministic rules were derived to perform the detection. In Ref. [21], wavelet transform for feature extraction is combined with a neural network for detection. The comparison with the present technique is not entirely consistent due to the following factors. The proposed methodologies were tested on three-phase transmission line models, and the average performance is shown in Table 5. In the case studies from the literature, only one model is utilised to benchmark the proposed methodologies. The testing technique utilised in this study is notably more complex due to the different system topologies and situations encountered by the fault diagnosis method. Furthermore, the proposed technique is limited to detecting transmission line fault current faults. Consequently, developing a single transmission line fault current detection model improves accuracy but with the cost of universal applicability. Finally, previous case studies isolate the feature extraction process and employ substantial expert knowledge to specify the appropriate features for fault diagnosis, whereas this research illustrates the CNN based on signal segmentation.

Although the results presented in the literature are not directly comparable to the tests performed in this research, they are put into context, and their fault detection accuracy is compared with other case studies. To address the first discrepancy in the comparison, the average detection accuracy is evaluated across all three parameters of three transmission line fault currents. Regarding fault detection, a CNN-based signal segmentation is recommended because it still performs

reasonably well despite the lack of specific feature extraction and the use of an integrated single network for fault identification. In Table 9, the reported detection rates (averaged across a large testing set) in Ref. [20] and Ref. [21] are utilised and compared to ideal, 20 dB, and 30 dB noise using CNN.

Table 9

Comparison of fault detection performance with alternative existing methods

Method	CNN (Ideal)	CNN (20dB noise)	CNN (30dB noise)	[20]	[21]
Detection accuracy (%)	99.11	99.36	99.39	97.89	98.67

The average performance of the developed technique over the three transmission line models is equivalent to that of the approaches provided in Ref. [20] and Ref. [21]. This comparison demonstrates that the overall performance is still comparable to strategies dedicated to specific network topologies while being evaluated over several network topologies without any unique tuning.

4. Conclusions

Even if the classic feature-based diagnostics continue to operate well and are more effective in many cases, finding optimal features in common practice is not easy. As an alternative to this traditional strategy, CNN for transmission line fault diagnosis appears feasible by avoiding some signal-processing steps. Such approaches decrease the time and effort required to develop effective signal-processing methods and feature extraction/selection procedures. Most deep learning research in transmission line fault detection has demonstrated remarkable viability by displaying excellent accuracy in model learning. However, the approaches have shown critical limitations in that the algorithms have been applied to the same data sets used to train their model. In practice, the fault can occur at any of its transmission lines, which may result in poor performance even with sophisticated algorithms. This study has focused on addressing this issue and demonstrated the importance of such effort for properly preparing input data.

A CNN for transmission line fault diagnosis based on a signal segmentation approach was presented in this paper. To accomplish this goal, signal segmentation was performed on a transmission signal by separating it into segments across each fault. The performance of the proposed method was evaluated by simulating various types of faults with different parameters, and the results obtained were encouraging. Compared with past research, the contributions of this paper can be summarised as follows.

- i. A new 1D-CNN architecture for transmission line fault classification is proposed. Without manually designed signal transformation or calculation as feature engineering, feature extraction and fault detection are achieved in a single model. By applying CNN-1D instead of CNN-2D as the classifier, the proposed architecture can avoid unnecessary and cumbersome structure changes of input data.
- ii. The 1D-CNN reduces the computation time, improves the speed of fault detection, reduces the influence of distribution network structure on the algorithm and realises the fault of the whole line without blind area.
- iii. The transmission line fault diagnosis based on the signal segmentation approach of CNN mainly benefits from the 1D-CNN of pooling and classifier layers by introducing the pooling layer, fully connected layer and SoftMax layer in the CNN construction process.

Acknowledgement

The authors acknowledge with gratitude the support and involvement of all parties, especially Universiti Teknologi MARA, Cawangan Pulau Pinang, for financial support in attending the 3rd ICISE 2023.

References

- [1] Aparna, A., Sabeena Beevi, Serene Benson, Ahamad Dilshad, and Deepa S. Kumar. "A modified CNN for detection of faults during power swing in transmission lines." In *2020 International Conference on Power, Instrumentation, Control and Computing (PICC)*, pp. 1-5. IEEE, 2020. <https://doi.org/10.1109/PICC51425.2020.9362482>
- [2] Huang, Ruiling, Hongbin Wang, He He, and Li Chen. "Fault diagnosis of short circuit in transmission line based on variational modal decomposition and whale algorithm." In *2021 3rd Asia Energy and Electrical Engineering Symposium (AEEES)*, pp. 130-135. IEEE, 2021. <https://doi.org/10.1109/AEEES51875.2021.9403227>
- [3] Davis, William Patrick. "Analysis of faults in overhead transmission lines." PhD diss., California State University, Sacramento, 2012.
- [4] Mustafa, Wan Azani, Haniza Yazid, and Mastura Jaafar. "A systematic review: Contrast enhancement based on spatial and frequency domain." *Journal of Advanced Research in Applied Mechanics* 28, no. 1 (2016): 1-8.
- [5] Chen, Yann Qi, Olga Fink, and Giovanni Sansavini. "Combined fault location and classification for power transmission lines fault diagnosis with integrated feature extraction." *IEEE Transactions on Industrial Electronics* 65, no. 1 (2017): 561-569. <https://doi.org/10.1109/TIE.2017.2721922>
- [6] Chua, Qing Shi, and Kai Chen Goh. "Transmission line fault detection: A review." *Indonesian Journal of Electrical Engineering and Computer Science* 8, no. 1 (2017): 199-205. <https://doi.org/10.11591/ijeecs.v8.i1.pp199-205>
- [7] Liu, Xinyu, Xiren Miao, Hao Jiang, and Jing Chen. "Data analysis in visual power line inspection: An in-depth review of deep learning for component detection and fault diagnosis." *Annual Reviews in Control* 50 (2020): 253-277. <https://doi.org/10.1016/j.arcontrol.2020.09.002>
- [8] Cai, Baoping, Yu Liu, and Min Xie. "A dynamic-Bayesian-network-based fault diagnosis methodology considering transient and intermittent faults." *IEEE Transactions on Automation Science and Engineering* 14, no. 1 (2016): 276-285. <https://doi.org/10.1109/TASE.2016.2574875>
- [9] Petrović, Ivica, Srete Nikolovski, Hamid Reza Baghaee, and Hrvoje Glavaš. "Determining impact of lightning strike location on failures in transmission network elements using fuzzy decision-making." *IEEE Systems Journal* 14, no. 2 (2019): 2665-2675. <https://doi.org/10.1109/JSYST.2019.2923690>
- [10] Jiang, Zhongyuan, Zhiwu Li, Naiqi Wu, and Mengchu Zhou. "A Petri net approach to fault diagnosis and restoration for power transmission systems to avoid the output interruption of substations." *IEEE Systems Journal* 12, no. 3 (2017): 2566-2576. <https://doi.org/10.1109/JSYST.2017.2682185>
- [11] Zhang, Xu, Shuai Yue, and Xiaobing Zha. "Method of power grid fault diagnosis using intuitionistic fuzzy Petri nets." *IET Generation, Transmission & Distribution* 12, no. 2 (2018): 295-302. <https://doi.org/10.1109/JSYST.2017.2682185>
- [12] Liu, Daobing, Xueping Gu, and Haipeng Li. "A complete analytic model for fault diagnosis of power systems." In *Zhongguo Dianji Gongcheng Xuebao(Proceedings of the Chinese Society of Electrical Engineering)*, vol. 31, no. 34, pp. 85-92. Chinese Society for Electrical Engineering, 2011.
- [13] Han, Ji, Shihong Miao, Yaowang Li, Weichen Yang, and Haoran Yin. "Fault diagnosis of power systems using visualized similarity images and improved convolution neural networks." *IEEE Systems Journal* 16, no. 1 (2021): 185-196. <https://doi.org/10.1109/JSYST.2021.3056536>
- [14] Paul, Debdyuti, and Subodh Kumar Mohanty. "Fault classification in transmission lines using wavelet and CNN." In *2019 IEEE 5th International Conference for Convergence in Technology (I2CT)*, pp. 1-6. IEEE, 2019. <https://doi.org/10.1109/I2CT45611.2019.9033687>
- [15] Jamil, Majid, Sanjeev Kumar Sharma, and Rajveer Singh. "Fault detection and classification in electrical power transmission system using artificial neural network." *SpringerPlus* 4, no. 1 (2015): 1-13. <https://doi.org/10.1186/s40064-015-1080-x>
- [16] Aparna, A., Sabeena Beevi, Serene Benson, Ahamad Dilshad, and Deepa S. Kumar. "A modified CNN for detection of faults during power swing in transmission lines." In *2020 International Conference on Power, Instrumentation, Control and Computing (PICC)*, pp. 1-5. IEEE, 2020. <https://doi.org/10.1109/PICC51425.2020.9362482>
- [17] Kim, Seokgoo, and Joo-Ho Choi. "Convolutional neural network for gear fault diagnosis based on signal segmentation approach." *Structural Health Monitoring* 18, no. 5-6 (2019): 1401-1415. <https://doi.org/10.1177/1475921718805683>

- [18] Xie, Yuan, and Tao Zhang. "Fault diagnosis for rotating machinery based on convolutional neural network and empirical mode decomposition." *Shock and Vibration* 2017 (2017). <https://doi.org/10.1155/2017/3084197>
- [19] Guo, Mou-Fa, Xiao-Dan Zeng, Duan-Yu Chen, and Nien-Che Yang. "Deep-learning-based earth fault detection using continuous wavelet transform and convolutional neural network in resonant grounding distribution systems." *IEEE Sensors Journal* 18, no. 3 (2017): 1291-1300. <https://doi.org/10.1109/JSEN.2017.2776238>
- [20] Roy, N., and K. Bhattacharya. "Identification and classification of fault using S-transform in an unbalanced network." In *2013 IEEE 1st International Conference on Condition Assessment Techniques in Electrical Systems (CATCON)*, pp. 111-115. IEEE, 2013. <https://doi.org/10.1109/CATCON.2013.6737482>
- [21] Dasgupta, Aritra, Sudipta Nath, and Arabinda Das. "Transmission line fault classification and location using wavelet entropy and neural network." *Electric Power Components and Systems* 40, no. 15 (2012): 1676-1689. <https://doi.org/10.1080/15325008.2012.716495>